CHEMICAL ENGINEERING TRANSACTIONS
VOL. 81, 2020
A publication of AIDIC
The Italian Association of Chemical Engineering
Online at www.cetjournal.it
Guest Editors: Petar S. Varbanov, Qiuwang Wang, Min Zeng, Panos Seferlis, Ting Ma, Jiří J. Klemeš

ISBN 978-88-95608-79-2; **ISSN** 2283-9216
DOI: 10.3303/CET2081212

Analysis of Factors Affecting Dropwise Condensation Heat Transfer Based on Theoretical Model

Jie Pang, Jinlan Gou, Chonghai Huang, Kai Chen, Qi Xiao, Shiwei Yao*

Science and Technology on Thermal Energy and Power Laboratory Wuhan, Hubei, China
crab2003@qq.com

Based on the processes of droplet nucleation, growth, coalescence and departure, the heat transfer model of dropwise condensation of a pure vapour on hydrophobic/superhydrophobic surfaces is developed. The influences of the number of nucleation site, minimum radius, contact angle and departure radius on heat transfer performance are studied by numerical simulation. The results indicate that the minimum radius affects the dropwise condensation a little while it is much less than the characteristic coalescence radius. The internal droplet thermal resistance increases as the contact angle increases. As a result, the heat transfer performance of superhydrophobic surfaces is not as good as that of hydrophobic surfaces.

1. Introduction

There are two forms of vapour condensation, i.e. filmwise condensation (FWC) and dropwise condensation (DWC). Schmidt et al. (1930) found dropwise condensation of which the heat transfer coefficient was several times or even dozens of times of filmwise condensation (Rose, 2002). Since then, dropwise condensation had been paid much more attention to scientific research and industrial application. Dropwise condensation contains the lifecycle of droplet nucleation, growth, coalescence and departure. The behaviour characteristic of droplets is the basis for understanding the law, build the physical model and predict the performance of dropwise condensation heat transfer.

Le Fevre and Rose (1966) first proposed a theoretical model of dropwise condensation heat transfer and used the droplet size distribution function fitted from experimental data. Based on assuming that the droplet size distribution stays the same, Wu and Maa (1976) built the population balance model and obtained the droplet size distribution of small droplets which have grown by direct condensation. Abu-Orabi (1998) combined the population balance model and droplet size distribution function, given a theoretical model of hemispherical droplets on a vertical surface. Kim and Kim (2011) extended Abu-Orabi's model to inclined superhydrophobic surfaces and derived the thermal resistance inside the droplet analytically. Miljkovic et al. (2013) obtained the droplet population distribution and heat flux of suspended and partial wetting droplets on superhydrophobic flat surfaces by considering the coalescence-induced droplet jumping. Hu and Tang (2014) introduced the circumferential angle in the calculation of departure radius and established the dropwise condensation heat transfer model of a horizontal tube. Parin et al. (2017) compared model parameters and numerical results of Le Fevre and Rose's model, Abu-Orabi's model and Kim and Kim's model, and found that the heat transfer coefficient was different, especially when the subcooling was lower.

In most industrial condensers, the air in the main heat exchange zone is very little and can be negligible. The droplets on hydrophobic/superhydrophobic surfaces will be fully wetted without air. The experimental results of vertical flat surfaces (Wang et al., 2010) and horizontal tube surfaces (Hu et al., 2015) showed that the hydrophobic surfaces had a better performance of dropwise condensation heat transfer while numerical simulation on flat surfaces (Kim and Kim, 2011) and horizontal tube surfaces (Hu and Tang, 2014) both had the opposite results. In this paper, the dropwise condensation heat transfer model at pure vapour environment is built. The factors affecting heat transfer performance are investigated by numerical simulation.

Paper Received: 04/06/2020; Revised: 05/07/2020; Accepted: 09/07/2020
Please cite this article as: Pang J., Gou J., Huang C., Chen K., Xiao Q., Yao S., 2020, Analysis of Factors Affecting Dropwise Condensation Heat Transfer Based on Theoretical Model, Chemical Engineering Transactions, 81, 1267-1272 DOI:10.3303/CET2081212

2. Heat transfer model

Consider a droplet with radius r on a plain surface with a hydrophobic coating which has fixed static contact angle θ, as shown in Figure 1, where T_s is the saturation temperature, T_{surf} is the substrate temperature, and δ is the coating thickness.

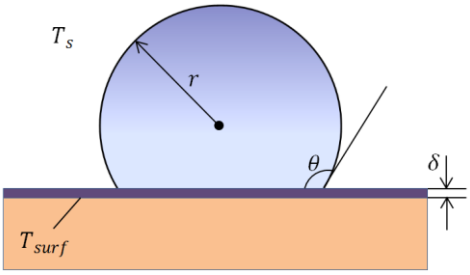

Figure 1: Droplet on a condensing surface with a hydrophobic coating

Considering the temperature drops due to vapour-liquid interfacial resistance, curvature resistance, thermal conduction through a droplet and thermal conduction through the coating layer, the heat transfer rate through a single droplet is

$$q_d = \frac{\pi r^2 (1 - r_{min}/r)\Delta T}{\frac{1}{2h_i(1-\cos\theta)} + \frac{r\theta}{4\lambda_l \sin\theta} + \frac{\delta}{\lambda_c \sin^2\theta}} \tag{1}$$

where r is the droplet radius, r_{min} is the minimum radius, ΔT is the total temperature difference or subcooling temperature between the vapour and the substrate, h_i is the interfacial heat transfer coefficient, θ is the contact angle, λ_l is the liquid thermal conductivity, δ is the coating thickness, and λ_c is the coating thermal conductivity. The minimum radius is expressed as:

$$r_{min} = \frac{2T_s\sigma_{lv}}{h_{fg}\rho_l \Delta T} \tag{2}$$

where σ_{lv} is the liquid-vapour interfacial tension, h_{fg} is the latent heat of vaporization, and ρ_l is the liquid density. Actually, the subcooling temperature ΔT in the above equation is the temperature difference between the vapour and the coating surface. The minimum radius will increase as the coating conductivity resistance increases. The interfacial heat transfer coefficient is:

$$h_i = \frac{2\alpha_c}{2-\alpha_c}\left(\frac{M}{2\pi R T_s}\right)^{1/2} \frac{h_{fg}^2 \rho_v}{T_s} \tag{3}$$

where α_c is the condensation coefficient and generally taken as unity, M is the molar mass of water, R is the molar gas constant, and ρ_v is the vapour density.
The droplet population distribution is:

$$\mathrm{N}(r) = \begin{cases} \dfrac{(r_{\max}/r_e)^{2/3} r (r_e - r_{\min})(A_2 r + A_3)}{3\pi r_e^3 r_{\max}(r - r_{\min})(A_2 r_e + A_3)} \exp(B_1 + B_2), & r < r_e \\ \dfrac{1}{3a r_{\max}^{1/3}} r^{-8/3}, & r \geq r_e \end{cases} \tag{4}$$

where parameters such as A_2, A_3 and so on can be referred in Kim and Kim (2011), r_e is the characteristic coalescence radius, r_{max} is the departure radius, a represents the ratio of the base area of the droplet to the radius squared, and $a = \pi$ when the droplet is hemispherical. When the droplet is not hemispherical, the former formula may have another form as:

$$\mathrm{N}'(r) = \frac{\mathrm{N}(r)}{\sin^2\theta} \tag{5}$$

Assuming that the nucleation sites form a square array, the characteristic coalescence radius is calculated by:

$$r_e = \sqrt{1/(4N_s)} \tag{6}$$

where N_S is the number of nucleation sites.
The departure radius is obtained by the force balance between surface tension and gravity:

$$r_{\max} = \left[\frac{6\sin\theta(\cos\theta_R - \theta_A)}{\pi(2 - 3\cos\theta + \cos^3\theta)} \frac{\sigma_{lv}}{\rho_l g} \right]^{1/2} \tag{7}$$

where θ_A is the advancing contact angle, θ_R is the receding contact angle, and g is the acceleration of gravity.
The area ratio covered by the base area of the droplets having a radius in the range of [$r_{\min}$, r] is:

$$\eta(r) = \int_{r_{\min}}^{r} \pi(r\sin\theta)^2 \mathrm{N}(r)dr, \quad \text{or} \quad \eta'(r) = \int_{r_{\min}}^{r} \pi(r\sin\theta)^2 \mathrm{N}'(r)dr \tag{8}$$

The dropwise condensation heat flux of the droplets having a radius in the range of [$r_{\min}$, r] is:

$$Q(r) = \int_{r_{\min}}^{r} q_d(r)\mathrm{N}(r)dr, \quad \text{or} \quad Q'(r) = \int_{r_{\min}}^{r} q_d(r)\mathrm{N}'(r)dr \tag{9}$$

3. Results and discussion

Based on the heat transfer model established in Section 2, the influences of the number of nucleation sites, minimum radius, contact angle and departure radius are investigated numerically by a Python code. The simulation parameters selected are mainly referred to Kim and Kim (2011).

3.1 Number of nucleation sites

The droplet population distribution and covered area ratio affected by the number of nucleation sites is shown in Figure 2, where the contact angle is 90 °, the advancing contact angle is 90 °, the receding contact angle is 80 °, the saturation temperature is 373 K, the wall subcooling temperature is 5 K, the coating thickness is 0.1 μm, and the coating thermal conductivity is 0.25 W m^{-1} K^{-1}. The minimum radius is 4.07 nm, and the departure radius is 0.904 mm by calculation. While the number of nucleation sites varies from 10^9 m^{-2} to 10^{12} m^{-2}, the characteristic coalescence radius is 15.8 μm, 5 μm, 1.58 μm and 0.5 μm. The population of small droplets increases while the number of nucleation sites increases, as shown in Figure 2a. The area occupied by the droplets having a radius in the range of [r, r+dr] is shown in Figure 2b. It can be seen that the droplets with a radius around the characteristic coalescence radius occupy more area. Based on Figure 2a, the area occupied by the small droplets increases while the number of nucleation sites increases. The area occupied by the droplets with radius in the range of [$r_{\min}$, r] increases, as shown in Figure 2c. The droplets will hold 79.3 % of the surface area as the number of nucleation sites is 10^9 m^{-2}, and increases to 92.6 % as the number of nucleation sites is 10^{12} m^{-2}.

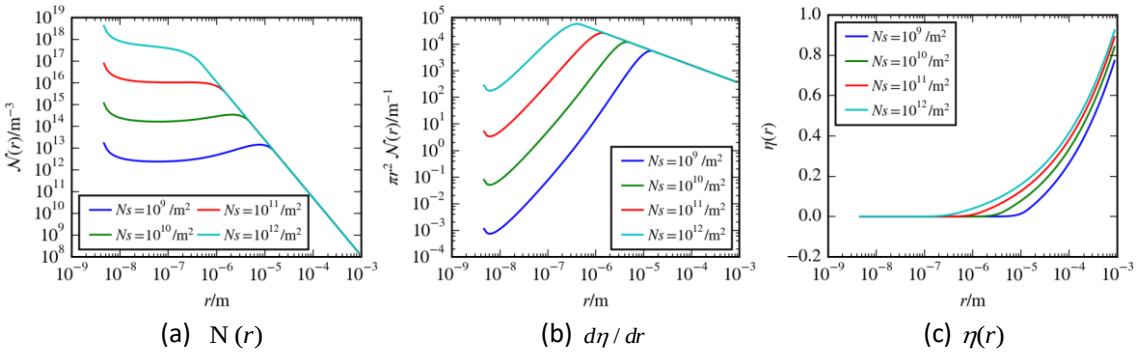

(a) $\mathrm{N}(r)$ (b) $d\eta/dr$ (c) $\eta(r)$

Figure 2: Population distribution and area ratio occupied by droplets at different numbers of nucleation sites

Heat flux affected by the number of nucleation sites is shown in Figure 3. Figure 3a shows the droplets with radius closed to the characteristic coalescence radius have a greater weight on heat transfer, and the performance of small droplets enhances while the number of nucleation sites increases. The overall heat flux is 99.92 kW m^{-2} as the number of nucleation sites is 10^9 m^{-2}, and it increases to 620.2 kW m^{-2} as the number of

nucleation sites is 10^{12} m^{-2}. These results indicate that the number of nucleation sites impacts on the heat transfer performance very significantly.

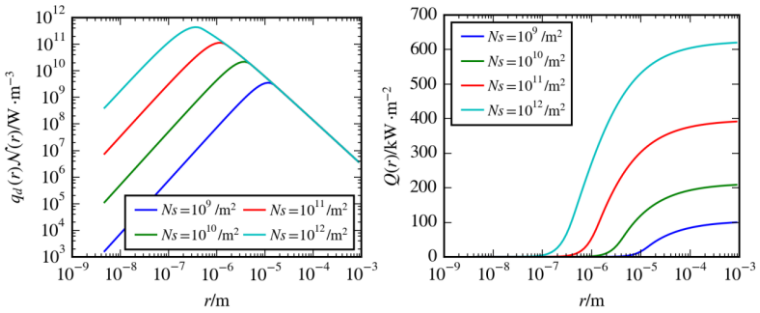

(a) dQ/dr (b) $Q(r)$

Figure 3: Heat flux at different numbers of nucleation sites

3.2 Minimum radius

Figure 4 shows the population distribution, covered area and heat flux at different minimum radius, where the number of nucleation sites is 10^{10} m^{-2}, the contact angle is 120 °, the advancing contact angle is 142 °, the receding contact angle is 102 °, the saturation temperature is 373 K, and the wall subcooling temperature is 10 K. At this case, the minimum radius calculated is 2.09 nm and set to 20.9 nm and 209 nm which are enlarged 10 times and 100 times. It can be seen in Figure 4a that due to a change of the minimum radius, the population distributions of small droplets are quite different. The droplets with a radius between the minimum radius and the characteristic coalescence radius have higher population while the minimum radius increases. As shown in Figure 4b, *dQ*/*dr* has a peak at the droplet radius of 3.4 μm, which is close to the characteristic coalescence radius of 5 μm, and much higher than 100 times of the minimum radius of 209 nm. As a result, the minimum radius affects the dropwise condensation heat transfer slightly. While increasing the minimum radius by a factor of 100, the overall heat flux declines by 2.4 %, as shown in Figure 4c.

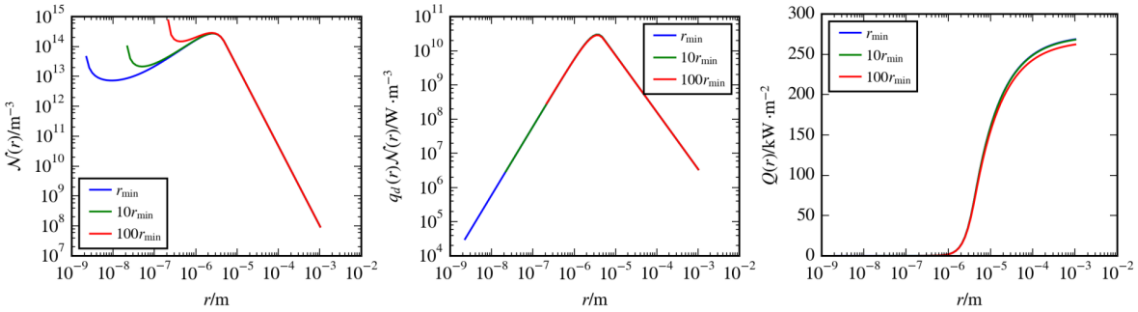

(a) $\mathrm{N}(r)$ (b) dQ/dr (c) $Q(r)$

Figure 4: Population distribution and heat flux at different minimum radius

3.3 Contact angle

Figure 5 shows the population distribution at different contact angles, where the contact angles are 90 °, 120 ° and 150 °, which are all 10 ° less than the advancing contact angle and 10 ° greater than the receding contact angle. The saturation temperature is 345 K, the wall subcooling temperature is 5 K, the coating thickness is 1 μm, the coating thermal conductivity is 0.2 W m^{-1} $K^{-1,}$ and the number of nucleation sites is 2.5×10^{11} m^{-2}. In this case, the departure radius is 1.32 mm, 0.88 mm and 0.47 mm. The population distributions have small difference while calculated by $\mathrm{N}(r)$. Due to the base area of the droplets decreases, while the contact angle is increasing, the covered area ratio is 90.11 %, 68.79 % and 22.28 %, as shown in Figure 6a. The population distributions are quite different while calculated by $\mathrm{N}'(r)$, and the covered area ratio is 90.11 %, 91.72 % and 89.14 %, as shown in Figure 6b. The area occupied by droplets while using $\mathrm{N}'(r)$ as the droplet population distribution is just the projected area while using $\mathrm{N}(r)$, which can be derived directly from Equation (5). It can be deduced that the reference Kim and Kim (2011) used $\mathrm{N}'(r)$ to simulate the droplet population distribution. Heat flux

affected by the contact angle is shown in Figure 6c. As the contact angle increases, for the droplets with the same radius, the heat transfer resistance becomes higher, and the population distribution changes a little, so the overall heat transfer performance declines. The heat flux is 151 kW m^{-2}, 121 kW m^{-2} and 57.2 kW m^{-2}. From the experimental results of pure vapour condensation (Wang et al., 2010), the heat flux of the superhydrophobic surface is only about 40 % of that of hydrophobic surface. Figure 6c agrees well with this and is different from some other numerical results both of flat surfaces (Kim and Kim, 2011) and horizontal tube surfaces (Hu and Tang, 2014). By inference, increasing the contact angle weakens the dropwise condensation heat transfer. Heat transfer enhanced by the superhydrophobic surface is mainly caused by the reduced departure radius with the presence of non-condensable gas.

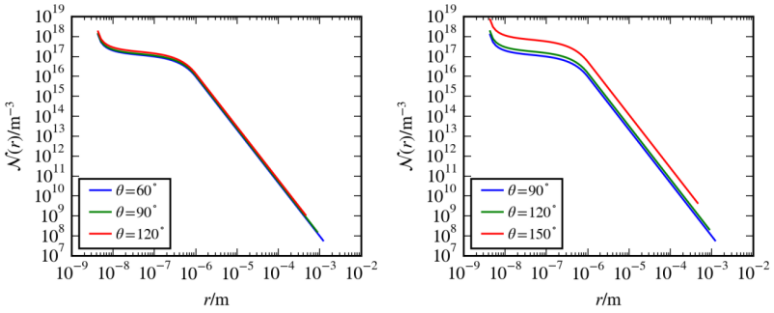

(a) $\mathrm{N}(r)$ (b) $\mathrm{N}'(r)$

Figure 5: Population distribution at different contact angles

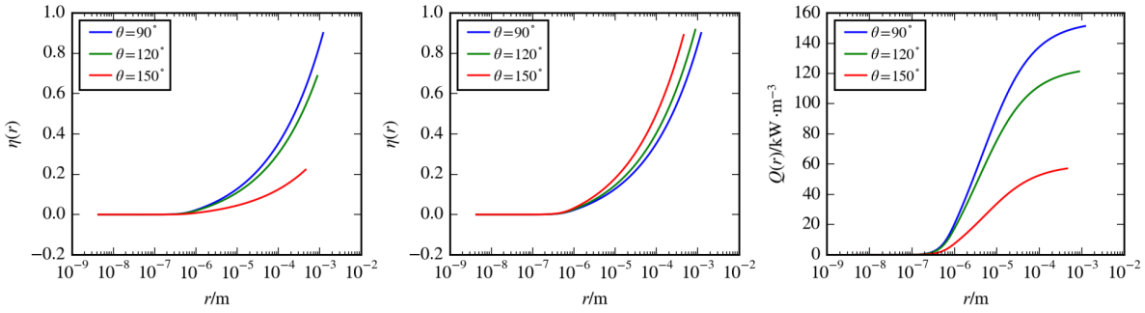

(a) $\eta(r)$ using $\mathrm{N}(r)$ (b) $\eta(r)$ using $\mathrm{N}'(r)$ (c) $Q(r)$ using $\mathrm{N}(r)$

Figure 6: Area ratio occupied by droplets and heat flux at different contact angles

3.4 Departure radius

The droplet population distribution and heat flux affected by the departure radius is shown in Figure 7, where the contact angle is 90 °, the advancing contact angle is 100 °, the receding contact angle is 80 °, the saturation is 373 K, the wall subcooling temperature is 10 K, the coating thickness is 1 μm, the coating

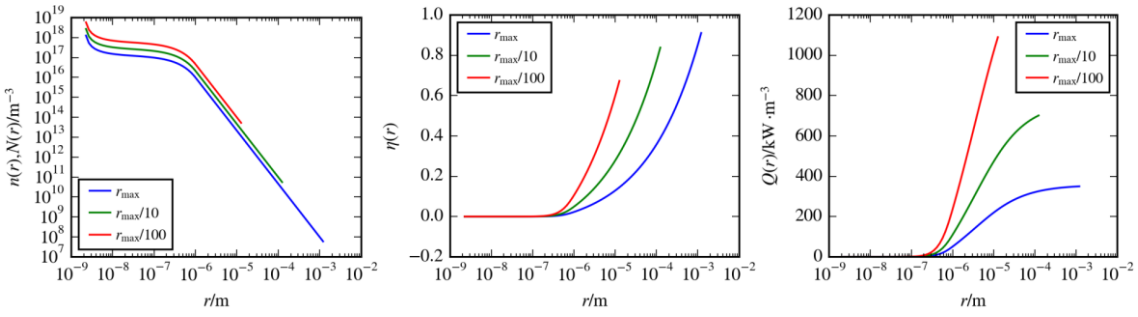

(a) $\mathrm{N}(r)$ (b) $\eta(r)$ (c) $Q(r)$

Figure 7: Population distribution and heat flux at different departure radius

thermal conductivity is 0.2 W m^{-1} $K^{-1,}$ and the number of nucleation sites is 2.5×10^{11} m^{-2}. The departure radius calculated is 1.28 mm, and set to 0.128 mm and 0.0128 mm to investigate its influence. As the departure radius decreases, the droplet population increases, the occupied area ratio decreases with the value of 91.08 %, 83.83 % and 67.25 %, and the overall heat flux increases obviously with the value of 350.2 kW m^{-2}, 703.0 kW m^{-2} and 1,093.9 kW m^{-2}. These results agree with the experimental results reported by Kim and Nam (2016).

4. Conclusions

(1) The number of nucleation sites affects the heat transfer performance of dropwise condensation very significantly. As the number of nucleation sites increases, the number of small droplets grows, the area occupied by droplets increases and the total heat transfer performance is greatly enhanced.
(2) Due to the presence of the coating conductivity resistance, the temperature difference between the vapour and the coating surface is less than that between the vapour and the substrate. The actual minimum radius will increase while the coating conductivity resistance increases. But the minimum radius affects the heat transfer performance slightly while it is much smaller than the characteristic coalescence radius.
(3) As the contact angle increases, the droplet population distribution has little difference, the resistance of the droplets with the same radius increases and the overall heat transfer performance descends. It can be concluded that the heat transfer performance of the superhydrophobic surface is poorer than that of the hydrophobic surface at the pure vapour environment.
(4) Dropwise condensation enhanced by the superhydrophobic surface is mainly because of the decreasing of the departure radius, with the proviso that the presence of non-condensable gas leads to droplets at suspended state.

Acknowledgements

The author wishes to thank the financial support from the National Natural Science Foundation of China (51706158).

References

Abu-Orabi M., 1998, Modeling of heat transfer in dropwise condensation, International Journal of Heat and Mass Transfer, 41(1), 81-87.
Hu H.W., Tang G.H., 2014, Theoretical investigation of stable dropwise condensation heat transfer on a horizontal tube, Applied Thermal Engineering, 62, 671-679.
Hu H.W. Tang G.H., Niu D., 2015, Experimental investigation of condensation heat transfer on hybrid wettability finned tube with large amount of non-condensable gas, International Journal of Heat and Mass Transfer, 85, 513-523.
Kim H., Nam Y., 2016, Condensation behaviors and resulting heat transfer performance of nano-engineered copper surfaces, International Journal of Heat and Mass Transfer, 93, 286-292.
Kim S., Kim K.J., 2011, Dropwise condensation modeling suitable for superhydrophobic surfaces, Journal of Heat Transfer, 133, 081502.
Le Fevre E.J., Rose J.W., 1966, A theory of heat transfer by dropwise condensation, Proceedings of 3rd International Heat Transfer Conference, 2, 362-375, DOI: 10.1615/IHTC3.180.
Miljkovic N., Engirght R., Wang E.N., 2013, Modeling and optimization of superhydrophobic condensation, Journal of Heat Transfer, 135(11), 111004.
Parin R., Penazzato A., Bortolim S., Del Col D., 2017, Modeling of dropwise condensation on flat surfaces, 13th International Conference on Heat Transfer, Fluid Mechanics and Thermodynamics, Portoroz, Slovenia, 91-96.
Rose J. W., 2002, Dropwise condensation theory and experiment: A review, Proceedings of the Institution of Mechanical Engineers, Part A: Journal of Power and Energy, 216, 115-128.
Schmidt E., Schurig W., Sellschopp W., 1930, Experiments on the condensation of water vapor in film and drop form, Tech. Mech. Thermodynamik, 1, 53-63 (In German).
Wang S.F., Lan Z., Wang A.L., Ma X.H., 2010, Dropwise condensation of steam and steam air mixture on super hydrophobic surfaces, CIESC Journal, 61(3), 607-611 (In Chinese).
Wu H.W., Maa J.R., 1976, On the heat transfer in dropwise condensation, Chemical Engineering Journal, 12, 225-231.